ACS NANO
Cite This: ACS Nano 2019, 13, 12090−12099
www.acsnano.org

ARTICLE

Tracking Airborne Molecules from Afar: Three-Dimensional Metal−Organic Framework-Surface-Enhanced Raman Scattering Platform for Stand-Off and Real-Time Atmospheric Monitoring

Gia Chuong Phan-Quang,[†] Ningchen Yang,[†] Hiang Kwee Lee,[†,‡] Howard Yi Fan Sim,[†] Charlynn Sher Lin Koh,[†] Ya-Chuan Kao,[†] Zhao Cai Wong,[†] Eddie Khay Ming Tan,[§] Yue-E Miao,[∥] Wei Fan,[∥] Tianxi Liu,[⊥] In Yee Phang,*[,#] and Xing Yi Ling*[,†]

[†]Division of Chemistry and Biological Chemistry, School of Physical and Mathematical Sciences, Nanyang Technological University, 21 Nanyang Link, Singapore 637371

[‡]Department of Materials Science and Engineering, Stanford University, Stanford, California 94305, United States

[§]Technospex Pte Ltd., 1092 Lower Delta Road, No. 04-01 Tiong Bahru Industrial Estate, Singapore 169203

[∥]State Key Laboratory for Modification of Chemical Fibers and Polymer Materials, College of Materials Science and Engineering, Innovation Center for Textile Science and Technology, Donghua University, 2999 North Renmin Road, Shanghai 201620, P.R. China

[⊥]Key Laboratory of Synthetic and Biological Colloids, Ministry of Education, School of Chemical and Material Engineering, Jiangnan University, 1800 Lihu Avenue, Wuxi 214122, Jiangsu, P.R. China

[#]Institute of Materials Research and Engineering, Agency for Science, Technology and Research (A*STAR), 2 Fusionopolis Way, Innovis, No. 08-03, Singapore 138634

Supporting Information

ABSTRACT: **Stand-off Raman spectroscopy combines the advantages of both Raman spectroscopy and remote detection to retrieve molecular vibrational fingerprints of chemicals at inaccessible sites. However, it is currently restricted to the detection of pure solids and liquids and not widely applicable for dispersed molecules in air. Herein, we realize real-time stand-off SERS spectroscopy for remote and multiplex detection of atmospheric airborne species by integrating a long-range optic system with a 3D analyte-sorbing metal−organic framework (MOF)-integrated SERS platform. Formed via the self-assembly of Ag@MOF core−shell nanoparticles, our 3D plasmonic architecture exhibits micrometer thick SERS hotspot to allow active sorption and rapid detection of aerosols, gas, and volatile organic compounds down to parts-per-billion levels, notably at a distance up to 10 m apart. The platform is highly sensitive to changes in atmospheric content, as demonstrated in the temporal monitoring of gaseous CO_2 in several cycles. Importantly, we demonstrate the remote and multiplex quantification of polycyclic aromatic hydrocarbon mixtures in real time under outdoor daylight. By overcoming core challenges in current remote Raman spectroscopy, our strategy creates an opportunity in the long-distance and sensitive monitoring of air/gaseous environment at the molecular level, which is especially important in environmental conservation, disaster prevention, and homeland defense.**

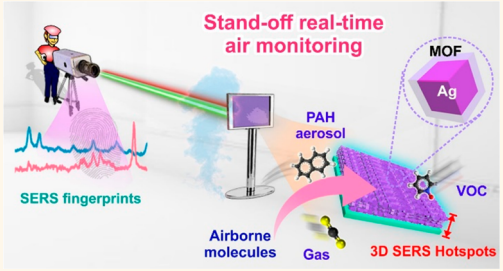

KEYWORDS: *stand-off detection, plasmonic nanoparticles, surface-enhanced Raman scattering, real-time monitoring, airborne sensing*

Stand-off Raman spectroscopy combines the advantages of both Raman spectroscopy and long-range detection to identify chemicals at distant and/or inaccessible sites,[1,2] providing an early indication of potential disasters and/or

Received: August 15, 2019
Accepted: September 13, 2019
Published: September 13, 2019

DOI: 10.1021/acsnano.9b06486
ACS Nano 2019, 13, 12090−12099

Scheme 1. Overview Schematic Display of Our Stand-Off MOF-SERS Platform for Real-Time Air Monitoring

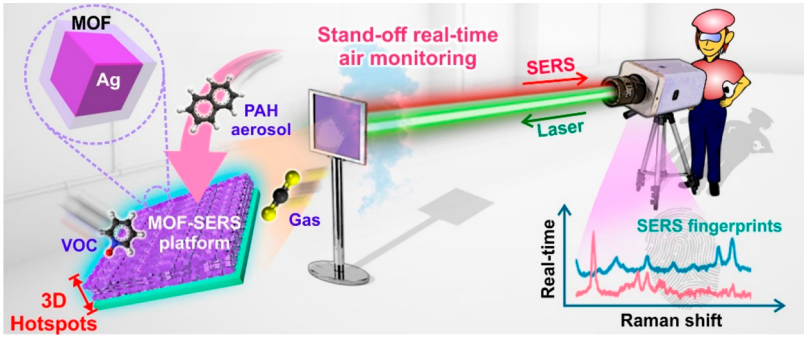

unhealthy air quality.[3,4] Typically performed at meter-range distances, stand-off Raman measurements give rise to molecular-specific vibrational fingerprints that can differentiate molecules of similar chemical structures and thus avert false signals.[5] It also benefits from no interference from water in the common fingerprint region between 600 and 1700 cm^{-1}, thereby highly appealing for outdoor detection even in humid conditions.[6] However, stand-off Raman suffers from intrinsically weak intensity (10^{-6} scattering probability) which is further aggravated with increasing distance (intensity $\propto 1/d^2$).[2,7] As such, current stand-off Raman detection is restricted to the detection of pure solids/liquids, and it is still not possible to detect diluted airborne species (such as gases and aerosols), even using high laser power (~400 mW) and long integration time (>1 min).[2,8] This weak sensitivity greatly hampers the use of stand-off Raman for remote threat/chemical detection and air quality monitoring because the majority of explosives, volatile organic compounds, and greenhouse gases exist in highly dispersed airborne conditions.[9]

Surface-enhanced Raman scattering (SERS) can potentially address the above problems by enhancing Raman signals of target airborne molecules by $>10^8$-fold when they are in close proximity to the surface of plasmonic nanostructures.[10−13] Using 2D plasmonic substrates of Ag and/or Au nanoparticles, ultrasensitive detections of small airborne molecules such as CO_2 and toxic aromatic compounds have been realized using lower operating laser power of tens of milliwatts.[4,14,15] Hence, we hypothesize that the integration of plasmonic-active platform with stand-off Raman spectroscopy can achieve an ultrasensitive stand-off SERS system to remotely detect airborne species. However, the facile coupling of conventional 2D SERS platforms and a stand-off Raman system remains a huge challenge owing to the following two main reasons. First, stand-off Raman system has large focal depth, typically in the range of millimeters to centimeters. When coupled with SERS, this large focal depth will be underutilized because most 2D SERS platforms, which are previously designed for microscopic Raman systems with submicrometer resolution, have nanometer thick plasmonic hotspot dimension along the *z*-direction.[12,16] Correspondingly, this inefficient utilization of stand-off laser excitation volume will lead to poor signal read-out due to the signal contribution from ambient interferences present in the laser volume. Second, current attempts in stand-off SERS rely on plasmonic particles that are unable to actively capture analytes from the air,[13] making it unsuitable for the detection of randomly dispersed airborne molecules that have no affinity to metal surfaces, especially in an open ambient environment. Hence, resolving both hotspot focal depth and poor analyte affinity issues are crucial to achieve rapid and univocal stand-off SERS detection of highly dynamic airborne species at the molecular level.

To accomplish this goal, we hereby develop a 3D multilayered Ag@MOF (MOF = metal−organic framework) core−shell particle platform that possesses micron-scale large hotspot depth and high analyte-sorbing ability. The MOF-SERS platform is then coupled with the stand-off Raman system for remote analyte detection to realize real-time stand-off SERS detection of multiplex airborne species, with sensitivity at the parts per billion (ppb) level at 2−10 m away (Scheme 1). Our platform displays superior sensitivity and response time in the detection of airborne chemicals over other Ag−MOF configurations, as demonstrated by the rapid recognition of aerosols and gases in 10 s. We also highlight the advantage of our platform in remote air-monitoring applications, as demonstrated by its ability to rapidly track chemical changes in atmospheric content when CO_2 gas is exposed to the platform in repeated cycles. By corroborating with principal component analysis (PCA), our robust stand-off SERS system achieves real-time and remote multiplex quantification of polycyclic aromatic hydrocarbons (PAH) mixtures even under the strong outdoor daylight background and ambient air. These valuable insights to realize ultrasensitive stand-off SERS detection are critical to expedite future application of long-range molecular detection in various important sectors including atmospheric/environmental sciences, disaster prevention, and homeland defense.

RESULTS AND DISCUSSION

In the fabrication of the 3D MOF-SERS platform, we employ Ag nanocubes (edge length, 121 ± 5 nm; Figure S1) as the plasmonic nanoparticle building blocks due to its strong SERS enhancement arising from their sharp tips and edges.[17,18] The Ag nanocubes are first treated with an ethanolic solution of hydrochloric acid to remove polyvinylpyrrolidone surfactant on as-synthesized Ag particles. This is to provide a featureless SERS background in the region of 600−1700 cm^{-1} which is necessary for accurate analyte detection. The Ag nanocubes are then encapsulated with a molecule-sorbing zeolitic imidazolate framework-8 (ZIF, Figure 1A(i), Figure S2, Experimental Methods)[19] due to the excellent ability of ZIF to concentrate a wide range of molecules (*e.g.*, bicyclic compounds) on the plasmonic surface for efficient SERS sensing.[4,19,20] Using a ZIF overgrowth method, we synthesize polycrystalline Ag@MOF particles with a continuous ZIF coating at a thickness of 44 ± 5 nm (Figure 1A(i), Figures S3 and S4).

Our 3D SERS platform is subsequently fabricated *via* the self-assembly of these Ag@MOF particles into a multilayered ensemble simply by drying a droplet containing 5 mg/mL of

DOI: 10.1021/acsnano.9b06486
ACS Nano 2019, 13, 12090−12099

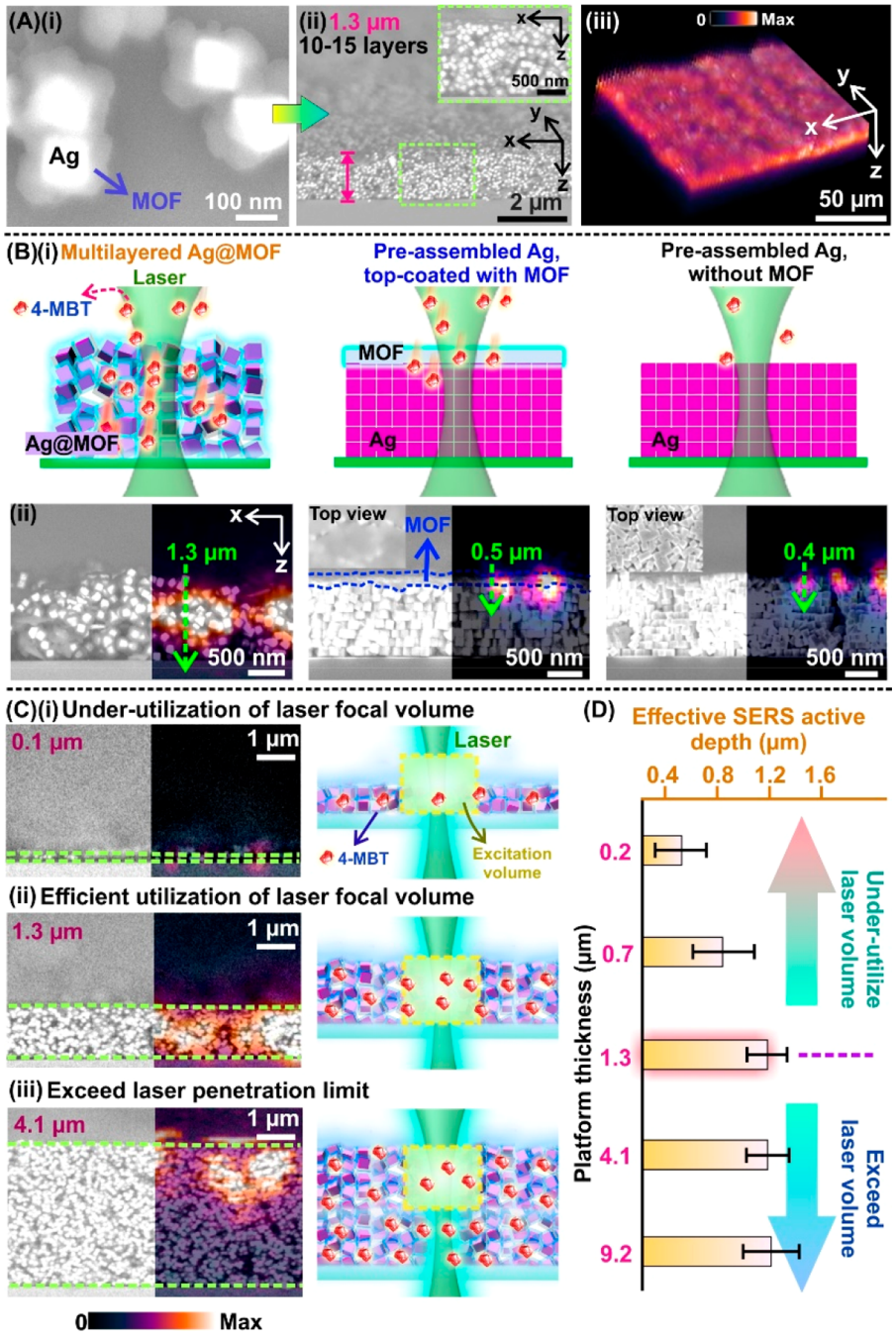

Figure 1. 3D MOF-SERS platform. (A) (i) SEM image showing Ag@MOF particles, (ii) cross-sectional SEM image showing the side view of multilayered Ag@MOF platform, and (iii) 3D $x-y-z$ SERS image of a segment of the platform (imaged with 20× objective lens). (B) (i) Schemes and (ii) cross-sectional SEM images showing the structure and how airborne molecules are absorbed and detected in different platform configurations. Half of the images in (ii) are overlapped with $x-z$ SERS hyperspectral images (imaged with 100× objective lens) showing the penetration of gaseous 4-MBT into the platform (Ag in the platforms has no 4-MBT surface groups prior to exposure). (C) (Left) SEM images overlapped with $x-z$ SERS images (imaged with 100× objective lens) of Ag@MOF platforms with increasing thickness and (right) schemes showing the hotspot and analyte density within the fixed laser focal volume where platforms of different thicknesses are used. (D) Effective SERS active depth and stand-off intensity (at 2 m) of 4-MBT's SERS band at 1077 cm^{-1} obtained from platforms with thickness ranging from 0.2−9.2 μm (using Ag pre-functionalized with 4-MBT).

Ag@MOF solution at ambient conditions.[21] The resulting platform is a 1.3 ± 0.2 μm thick (10−15 layers) close-packed assembly of multiple Ag cores within a collective MOF shell structure (Figure 1A(ii), Figure S4) with an interparticle distance of <10 nm. Such a small interparticle distance is commonly observed in hard-core soft-shell structures[22] and is advantageous for our subsequent SERS application because it allows strong plasmonic coupling among neighboring Ag cubes to form intense SERS hotspots for ultrasensitive sensing.[11] We then characterize our 3D Ag@MOF platform in terms of its SERS hotspots using confocal Raman microscopy. We employ 4-methylbenzenethiol (4-MBT) as the probe molecule due to its strong and distinct vibrational fingerprints at 1077 cm^{-1} (ν_{CS}, β_{CCC}, Figure S5) for SERS characterization/imaging. Hyper-

DOI: 10.1021/acsnano.9b06486
ACS Nano 2019, 13, 12090−12099

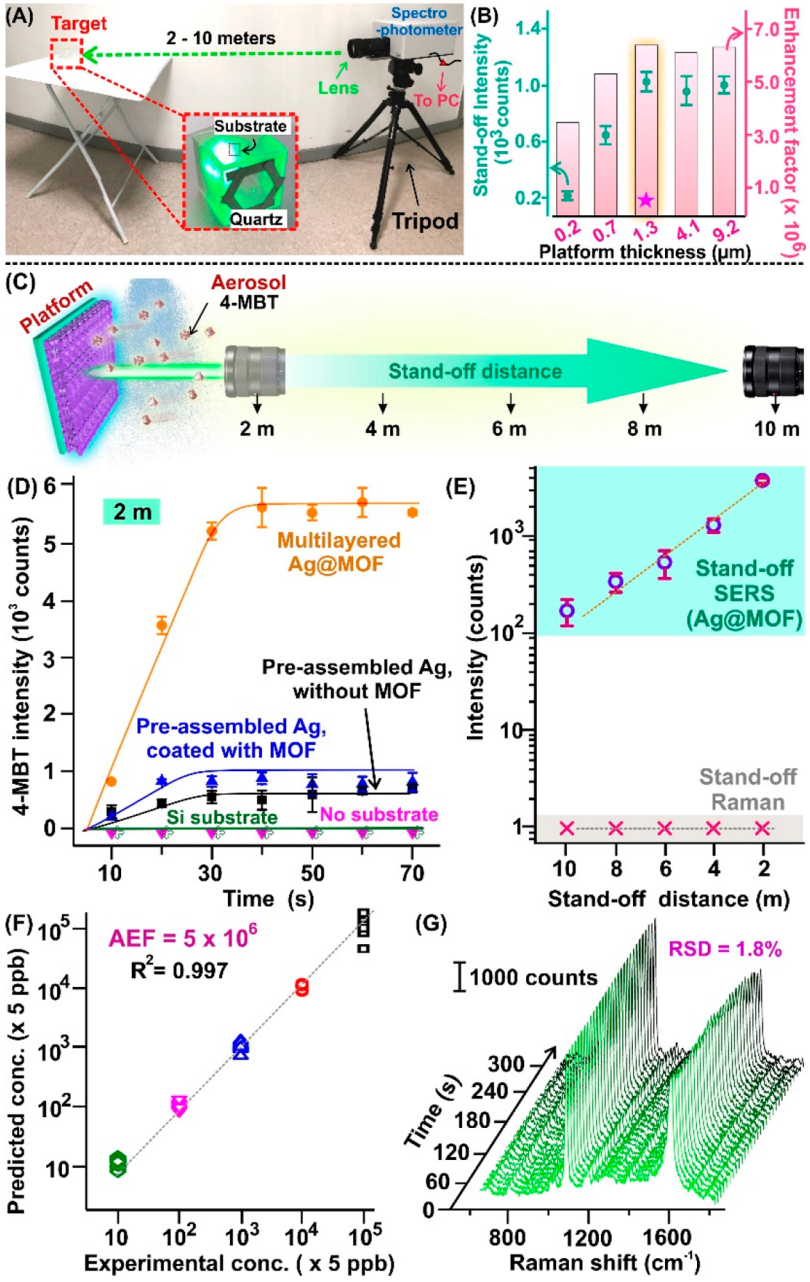

Figure 2. Stand-off SERS using 3D MOF-SERS platform. (A) Set-up of our stand-off SERS system. (B) Stand-off intensity (at 2 m) of 4-MBT's 1077 cm^{-1} obtained from platforms of thickness ranging from 0.2−9.2 μm (with Ag pre-functionalized with 4-MBT). (C) Scheme showing the stand-off SERS detection of aerosolized 4-MBT (500 ppm, Ag in the platforms has no 4-MBT surface groups). (D) Real-time 4-MBT intensity obtained in the stand-off SERS detection using different platforms. (E) 4-MBT intensities obtained at distances from 2 to 10 m using our Ag@MOF SERS platform and normal Raman detection. (F) Partial least-squares calibration graph of different 4-MBT airborne concentrations detected using our stand-off SERS system (at 2 m). (G) Consistent real-time stand-off SERS spectra of 4-MBT recorded on Ag@MOF substrate for a continuous period of 300 s after the substrate has reached saturation.

spectral $x-y-z$ SERS imaging reveals the 3D SERS active volume of our multilayered platform (Figure 1A(iii)), clearly indicating that plasmonic hotspots are intense and distributed homogeneously over all spatial directions. It is noteworthy that the relative standard deviation (% RSD) of SERS intensity using our 3D Ag@MOF platform is only <9% over a large $x-y$ area of several mm^2 and <10% along its $x-z$ plane (Figure S6). To the best of our knowledge, our assembly methodology produces the largest and thickest homogeneous 3D SERS platform which offers large plasmonic hotspot volume to fully exploit the millimeter-scale excitation volume in stand-off Raman systems essential for sensitive molecular read-out.[21]

To illustrate the superior analyte-sorbing capability of our platform, we compare it with two other common 3D SERS platforms, *i.e.*, (1) pre-assembled Ag nanocubes top-coated with a MOF layer (~200 nm) (see the Supporting Information, substrate 2) and (2) pre-assembled Ag nanocubes without MOF (see the Supporting Information, substrate 3). Briefly, both SERS platforms are initially exposed to gaseous 4-MBT for 2 h and subsequently analyzed by tracking the signature 4-MBT signal along the z-direction to determine the penetration depth

DOI: 10.1021/acsnano.9b06486
ACS Nano 2019, 13, 12090−12099

of analyte molecules into respective platforms upon saturation (Figure 1B, Figure S7). Using 4-MBT's characteristic band at 1077 cm^{-1}, we observe that the Ag@MOF platform allows the deepest analyte penetration with a depth of 1.3 ± 0.1 μm, as determined by the full-width half-maximum (fwhm) of the SERS intensity−distance profile scanned along the $x-z$ plane. In contrast, the two control platforms exhibit >2-fold shorter penetration depths at ∼0.5 ± 0.1 μm (Figure S7, Supporting Information 1). These observations affirm that the multilayered Ag@MOF is able to sorb the analyte molecules more efficiently, thereby giving higher apparent penetration depth. We attribute the better performance of the multilayered Ag@MOF platform to its porous and more homogeneous distribution of the analyte-sorbing MOF moiety throughout the whole platform, which allows airborne molecules to populate the entire 3D hotspot volume. On the other hand, Ag assembly top-coated with MOF does not possess MOF moiety throughout its z-direction, and it can only sorb molecules at its top layer. The bare Ag assembly without MOF platform does not have any analyte capturing ability and only relies on chemisorption of 4-MBT molecules on Ag surfaces. Such excellent analyte-sorbing ability of the multilayered 3D Ag@MOF configuration is crucial to accumulate a high density of analyte molecules within the large stand-off laser excitation volume for ultrasensitive SERS read out.

Upon affirming the optimal MOF-SERS configuration for efficient analyte capture, we further tune the thickness of our multilayered 3D Ag@MOF platform to maximize analyte signals for ultrasensitive and reliable molecular detection. To evaluate the optimal thickness of Ag@MOF particle ensemble, we pre-modified Ag surfaces with 4-MBT and perform $x-z$ hyperspectral SERS imaging on various MOF-SERS platforms with thickness ranging from ∼0.2 ± 0.1 μm (1−2 layers) to 9.2 ± 0.8 μm (40−45 layers, Figure 1C, Figure S8). We determine the effective SERS-active depth using the fwhm value of SERS intensity-distance profile obtained during $x-z$ SERS imaging. Notably, the SERS-active depth, also average SERS intensity, increases from 0.5 to 1.2 μm as the physical platform's thickness increases from 0.2 μm (1−2 layers) to 1.3 μm (10−15 layers). The hotspot thickness and SERS intensity eventually plateau at ∼1.2 μm (Figure 1D, Figure S8) even when the platform's thickness increases beyond 1.3 μm. The plateau in SERS-active depth and intensity is probably due to limited laser penetration depth through the close-packed assembly nanocubes, as commonly reported in multilayered platforms.[23,24] Nevertheless, our results evidently highlight the importance of thicker SERS platforms and larger SERS hotspot volume to better utilize the laser excitation volume as compared to thin platforms (Figure 1C). From here onward, we use the best performing 3D multilayered Ag@MOF platform with optimal thickness of 1.3 μm (10−15 layers) for our subsequent stand-off detection demonstrations.

We realize stand-off SERS detection by integrating our 3D Ag@MOF platform with a stand-off Raman system with large collection volume of 1 mm × 1 mm × 3.9 mm in x-, y-, and z-axes, respectively (Figure 2A, Figure S9). We begin by positioning our stand-off Raman system at a distance of 2 m (which is also our standardized distance used for demonstrations, unless otherwise stated) and measure 4-MBT signals across all Ag@MOF platforms of various thicknesses. Notably, we observe a ∼5-fold increase in intensity when the MOF-SERS platform thickness increases from 0.2 to 1.3 μm (237 ± 30 counts to 1041 ± 150 counts), which corresponds to an increment of stand-off SERS enhancement factor (EF) from 3.5 × 10^6 to 6.4 × 10^6 (Figure 2B, Supporting Information 2). The stand-off SERS signal intensity and calculated EF plateau at ∼1000 counts and ∼6.2 × 10^6, respectively, as the platform thickness increases further from 1.3 to 4.1 μm and 9.2 μm. This stand-off result is in agreement with the aforementioned trend in confocal SERS imaging, affirming that the optimal thickness for multilayered Ag@MOF platform is 1.3 μm, equivalent to 10−15 layers of Ag@MOF nanoparticles. Overall, our finding indicates that thick Ag@MOF platforms with micron-size hotspot volume are essential to maximize the hotspot population within the laser collection volume and further boost the SERS intensity of target molecules.

Importantly, our 3D Ag@MOF platform is able to swiftly capture and identify airborne molecules at a stand-off distance, providing real-time monitoring of atmospheric changes to allow prompt remediation to be taken. We demonstrate the ability to detect airborne species of our platform by introducing aerosolized 4-MBT (500 ppm) near the SERS platform and concurrently measure the time-dependent and stand-off SERS responses from the analyte molecules. It is noteworthy that this experiment is performed using Ag nanocubes cleaned with HCl and not with Ag particles that are pre-modified with 4-MBT. This is to ensure a more accurate evaluation on the overall sorption kinetics of Ag@MOF ensemble (Figure 2C). Our multilayered Ag@MOF platform rapidly records 4-MBT SERS signature within 10 s, which gradually reaches an intensity of >5000 counts within 30 s (Figure 2D) of aerosol exposure. In contrast, control platforms comprising of pre-assembled Ag top-coated with MOF and pre-assembled Ag without MOF exhibit 6-fold poorer signals within similar time periods of 30 s (Figure 2D). Using a Lagergren pseudo-first-order adsorption kinetics,[25] we find that the multilayered Ag@MOF platform displays the highest sorption constant of $k = 5.5 \times 10^{-2}$ s^{-1}, which is 10-fold higher than the other control platforms (Supporting Information 3). This observation again demonstrates the better analyte sorptivity and corresponding SERS sensitivity of multilayered Ag@MOF platform over other platform configurations toward the detection of airborne species in both aerosolized and gaseous forms (Figure S10). It is also noteworthy that no signal is detected in the absence of plasmonic particles, indicating that normal stand-off Raman detection is inapt for airborne analyte detection (Figure 2D). Collectively, both stand-off and confocal Raman microscopic experiments are in close agreement and jointly affirm that multilayered Ag@MOF with 1.3 μm thickness is the optimal 3D SERS platform essential for remote molecular sensing.

We also highlight that the detection can be performed at further stand-off distances, exemplifying the potential of our strategy in the real-life detection tasks at border, river, or mountainous geographical areas. Our platform exhibits 4-MBT signals at extended stand-off distances from 2 m up to 10 m and outperforms the normal Raman detection at every distance (Figure 2E, Figure S11). While the signal intensity decreases with distance (Raman intensity $\propto 1/d^2$), it is noteworthy that we are using 8-fold lower laser power (≤55 mW) than other common stand-off Raman techniques with ultrahigh laser power of >400 mW.[2,7] This feature is a significant advancement in stand-off Raman spectroscopy, especially in enhancing safety for operator's eye and skin. Moreover, the platform can detect down to 50 ppb of aerosolized 4-MBT, at which we observe >100 counts of distinct 4-MBT's vibrational signature at 1077 cm^{-1} (Figure S12). This detection limit corresponds to a high

DOI: 10.1021/acsnano.9b06486
ACS Nano 2019, 13, 12090−12099

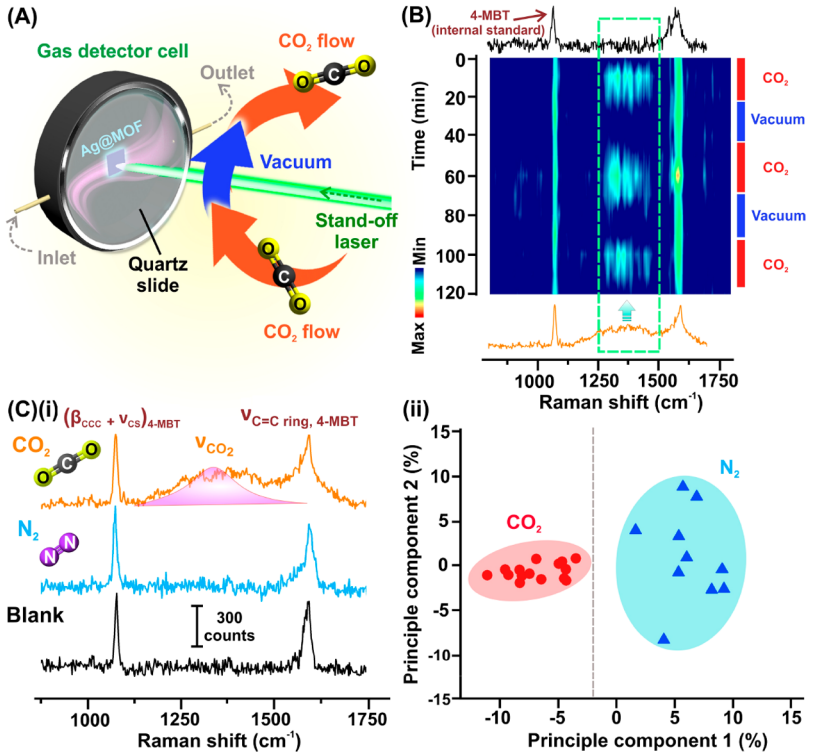

Figure 3. Remote SERS-based gas detector. (A) Scheme showing remote tracking of CO_2 in real time for several cycles using multilayered Ag@MOF platform. (B) Time-resolved SERS intensity profile of 1360 cm^{-1} band, showing the absorption and detection of CO_2 in several cycles. (C) (i) Spectroscopic observation of CO_2 vibrational modes (shown with respect to internal standard peak of 4-MBT grafted on the Ag particle) in the detection of CO_2, which is not observed in the control experiments with N_2 flow and no gas (blank), (ii) Principle component analysis (PCA) score plot of stand-off SERS spectra observed in the presence of CO_2 or N_2.

analytical enhancement factor (AEF) of 5×10^6 (Figure S13, Supporting Information 4). Importantly, the SERS spectra collected across different concentrations from 500 ppm to 50 ppb enable us to construct a standard calibration curve using partial least-squares (PLS) regression. This in turn allows subsequent quantification of analyte concentration (Figure 2F). The calibration curve exhibits a 0.997 linear coefficient, highlighting our stand-off SERS design as a reliable platform to identify and quantify highly dispersed molecules in air. Furthermore, we observe stable and consistent signal intensity (relative standard deviation in intensity is $\lesssim$1.8%) for a continuous period of 300 s after the platform has been saturated with 4-MBT molecules (Figure 2G). This clearly indicates that both the Ag@MOF SERS platform and the stand-off instrument are highly robust and not affected by external disturbances, such as air perturbation, that could potentially contribute to intensity fluctuation during prolonged measurements. By combining analyte-sorbing MOF scaffold and dense 3D plasmonic hotspot, our integrated approach resolves the bottleneck in stand-off Raman detection to enable the quantification of airborne molecules up to 10 m away, even at low laser power of $\lesssim$55 mW,

One potential application of our 3D Ag@MOF platform is its use as a highly responsive remote air monitoring device to provide real-time readout of specific vibrational fingerprints of small gaseous molecules that do not have specific affinity with the metal surface. Commercial air-monitoring devices installed in households and buildings rely heavily on a photoelectric method that does not provide molecular fingerprints, is prone to false alarms, and usually requires >15 min to recognize abnormal air composition.[26,27] As a proof of concept, we demonstrate the remote and real-time SERS sensing of gaseous carbon dioxide (CO_2) with high molecular specificity and showcase the potential of our platform as an ideal alternative to conventional detectors. Our 3D SERS platform is positioned within a gas flow cell that is connected to a CO_2 source (50 sccm and 1 atm), and SERS signals are recorded in consecutive CO_2–vacuum cycles (Figure 3A). In this demonstration, the Ag surface is pre-modified with 4-MBT as the internal standard, whereby all spectra are standardized against 4-MBT's 1077 signals to eliminate signal fluctuations (Figure 3B). We choose 4-MBT as our internal standard because it can bond to the Ag surface *via* a strong Ag–S covalent bond and, thus, does not undergo detachment/reattachment during evacuation and provides a consistent signal. As CO_2 exposure increases, we note the emergence of a broad SERS band centered at 1360 cm^{-1} rapidly within $\lesssim$5 min (Figure 3B). Notably, this broad band diminishes as soon as the cell is evacuated under vacuum. Repetitive appearance and disappearance of the 1360 cm^{-1} band is observed when the Ag@MOF SERS platform is subjected to continuous cycling between CO_2 flow and vacuum evacuation, respectively. This observation clearly denotes the high reversibility of the sorption and desorption of CO_2 gas molecules in our 3D Ag@MOF platform, a feature critical for application in real-time and reusable stand-off SERS monitoring of airborne species. In contrast, control experiment involving nitrogen gas (N_2) does not exhibit any vibrational feature near the 1360 cm^{-1} region (Figure 3C). Principle component analysis (PCA, an analysis to differentiate spectra based on algorithms applied on their spectral features) further affirms that SERS signatures obtained when exposing Ag@MOF to CO_2 or N_2 are statistically different. We therefore attribute the SERS band centered at 1360 cm^{-1} to the symmetric stretching mode of

DOI: 10.1021/acsnano.9b06486
ACS Nano 2019, 13, 12090–12099

CO_2 (ν_{CO2}) molecules accumulated at the solid-MOF interface.[14] Our approach thus offers a rapid and molecular-specific recognition of small gas molecules to prevent/minimize false positive using their specific vibrational fingerprints, even for molecules that do not have specific affinity with metal surface. Moreover, our stand-off SERS detection gives real-time results without tedious air sampling procedures, which is a significant advantage over conventional sensors which require preconcentration of gas molecules using electrodeposition[10] or ultralow temperature (−80 °C).[28]

In addition, we would like to emphasize that the ability to absorb and desorb concentrated airborne molecules depends on the types of molecules and their affinity toward the Ag surface. Small gaseous molecules with low affinity to Ag, such as CO_2, can be desorbed from the Ag@MOF system *via* vacuum and heat activation, and the substrate can be reused for another detection. Bigger molecules like naphthalene and toluene can be trapped within the MOF network and harder to be completely removed. On the other hand, molecules with high affinity to the Ag surface, such as 4-MBT that can form a Ag−S covalent bond, remain on the Ag surface upon absorption. Hence, for the two latter cases, the substrates should be for one-time use only.

To simulate a real-life multiplex sensing scenario in air quality monitoring, we perform a series of outdoor detections of aerosolized mixtures of (poly)cyclic aromatic hydrocarbons (PAH), naphthalene, and toluene (Figure 4A,B), which are major pollutants commonly found in haze.[29] We first construct a signal-to-concentration calibration under controlled laboratory conditions for various mixture compositions of naphthalene (Nap) and toluene (Tol), ranging from Nap/Tol 15:85 (mol/mol, airborne concentration 850:3500 ppm, respectively) to Nap/Tol 1:99 (49:3500 ppm) (Supporting Information 5, Figure S14). By introducing the aerosol mixture in the vicinity of the Ag@MOF platform, we are able to collect multiplex spectra exhibiting characteristic vibrational fingerprints of each analyte within 10 s. We observe the SERS bands of naphthalene at 763 cm^{-1} (δ_{CH}) and 1380 cm^{-1} (ν_{C-C}), as well as toluene signatures at 786 cm^{-1} (δ_{CH}) and 1004 cm^{-1} (symmetric $\nu_{C-C\ (ring)}$) in different intensity ratios according to the mixture composition (Figure S14A). For instance, the intensity ratio of Nap (763 cm^{-1})/Tol (786 cm^{-1}) increases from (0.12 ± 0.05) to (0.86 ± 0.1) as we increase the Nap/Tol ratio from 1:99 to 15:85 (Figure S14), respectively. Such spectral features enable the accurate quantification of each component content within the multiplex detection, as shown in our predicted PLS model and PCA score plot (Figure S14C, Figure S15). These results demonstrate that we are able to remotely measure the concentration of airborne molecules down to tens of ppm level, which is also the permitted threshold set by the Occupational Safety and Health Administration (OSHA).[18]

More importantly, we further exploit the multiplexing capability of our stand-off SERS system to remotely identify and quantify PAH composition in an outdoor setting under strong daylight intensity during afternoon time. Real-time SERS spectra evidently display the signature vibrational signals of target molecules amidst the background interference (Figure 4C,D, Figure S16). Upon background subtraction and baseline correction, the outdoor spectra of Nap/Tol 15:85 and 5:95 samples match well with the calibration spectra, whereby the relative intensity ratio of Nap/Tol SERS bands at 763 cm^{-1}/786 or 1380 cm^{-1}/1004 cm^{-1} are tallied with the calibration graph (Figure 4E, Figure S17). This result clearly showcases a high-performance stand-off SERS sensor capable of remotely

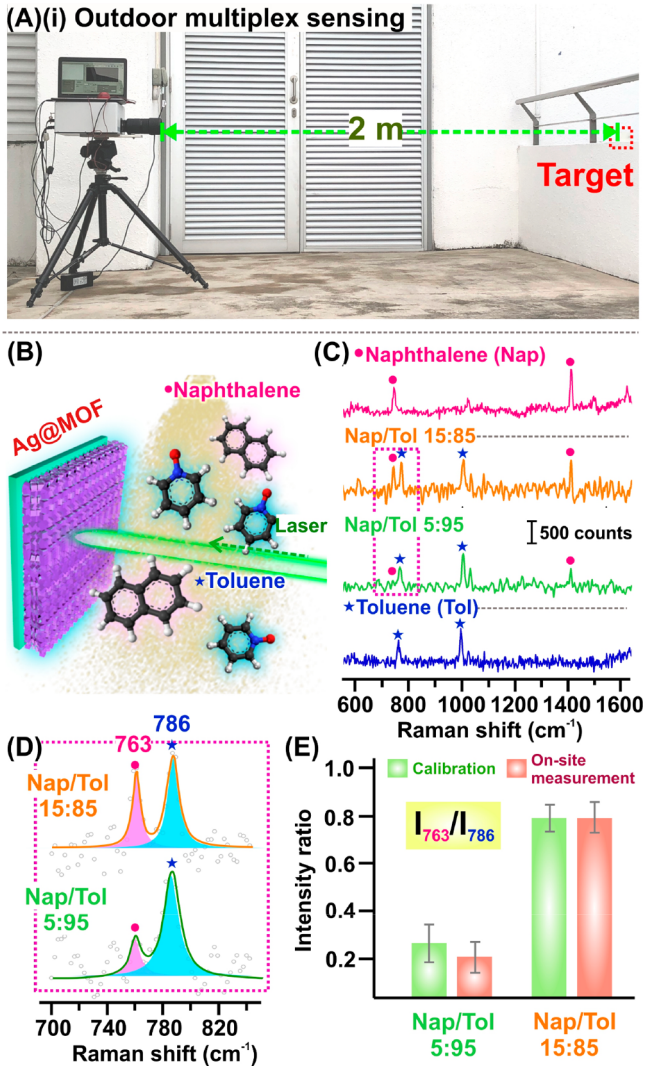

Figure 4. Outdoor remote sensing of airborne polycyclic aromatic hydrocarbon (PAH) mixture. (A) (i) Outdoor stand-off detection setup. (B) Scheme showing the stand-off detection of aerosolized toluene and naphthalene. (C) Stand-off multiplex spectra obtained in outdoor condition with natural light, for Nap/Tol 5:95 and 15:85 mixture, with reference to individual naphthalene and toluene SERS spectra. (D) Spectral analysis of characteristic signals of the analytes within the dotted region in (C). (E) Comparison of Nap/Tol signal intensity ratio between calibration spectra and outdoor spectra, using 763 and 786 cm^{-1} signals.

quantifying multiple airborne species in both laboratory-based and outdoor environments at high accuracy. The stand-off SERS system allows rapid sorption and identification of foreign molecules in the atmosphere, so that timely and adequate actions can be promptly taken in the event of adverse weather, disaster, and terrorism while ensuring the safety of operators.

CONCLUSIONS

In conclusion, we have achieved real-time stand-off SERS detection of airborne molecules by integrating stand-off Raman with a 3D Ag@MOF platform possessing micron-scale hotspot volume and high molecule sorbing ability. Our stand-off SERS system enables rapid quantitative detection of aerosolized chemicals with parts per billion (ppb) detection limit at a remote distance of 2−10 m. We are also able to achieve real-time stand-

DOI: 10.1021/acsnano.9b06486
ACS Nano 2019, 13, 12090−12099

off monitoring of small gas molecules in multiple on−off cycles, exemplifying the potential application of our platform in prolonged atmospheric monitoring. Notably, the stand-off 3D SERS system can rapidly elucidate the fingerprints of multiple airborne polyaromatic hydrocarbons in an outdoor environment, even under strong daylight background interference. These collective advantages of our stand-off SERS system tackle the current limitations in remote Raman spectroscopy, and create a paradigm shift for the applications in atmospheric/environmental sciences, disaster prevention, and homeland defense.

EXPERIMENTAL METHODS

Chemicals. Silver nitrate (≥99%), anhydrous 1,5-pentanediol (PD, ≥97%), poly(vinylpyrrolidone) (PVP, average MW = 55000), decane (≥98%), zinc nitrate hexahydrate (reagent grade, 98%), 2-methylimidazole (99%), 1*H*,1*H*,2*H*,2*H*-perfluorodecanethiol (PFDT; 97%), methylbenzenethiol (4-MBT, 98%), naphthalene (99%), and 1-propanol (anhydrous, 99.7%) were purchased from Sigma-Aldrich; copper(II) chloride (≥98%) was from Alfa Aesar; methanol (ACS reagent, ≥ 99.8%) was from J.T. Baker; ethanol (ACS, ISO, Reag. Ph Eur) and ammonia (ACS, Reag. Ph Eur) were from EMSURE; dimethylformamide (HPLC grade) was obtained from Fisher Scientific; nitrogen (N_2; ALPHAGAZ 1; 99.999%) and carbon dioxide (CO_2; ALPHAGAZ 1; 99.99%) were purchased from Singapore Oxygen Air Liquide Pte Ltd. All chemicals were applied without further purification. Milli-Q water (>18.0 MΩ. cm) was purified with a Sartorius Arium 611 UV ultrapure water system.

Determining the Laser Focal Depth of Stand-off Instruments. A substrate of 100 nm fluorescent microspheres is positioned at 2 m from the stand-off instruments, and the substrate is then moved along the *z*-axis forward and backward a few centimeters from the original position. The full-width half-maximum of the intensity profile is then obtained.

Synthesis and Purification of Silver Nanocubes. The preparation of Ag nanocubes was synthesized in high yield *via* the polyol method described in the literature.[1] Briefly, 10 mL of copper(II) chloride (8 mg/mL), poly(vinylpyrrolidone) (20 mg/mL), and silver nitrate (20 mg/mL) were separately dissolved in 1,5-pentanediol. The chemicals were sonicated and vortexed repeatedly to dissolve them. A 35 μL portion of copper(II) chloride solution was then added to the silver nitrate solution. Then, 20 mL of 1,5-pentanediol in a 100 mL round bottomed flask was heated to 190 °C for 10 min. A 250 μL portion of poly(vinylpyrrolidone) precursor was added to flask dropwise every 30 s, while 500 μL silver nitrate precursor was injected every minute using a quick addition. The addition process continued until the greenish coloration of the reaction mixture faded off.

For the purification of Ag nanocubes, 1,5-pentanediol was first removed from the mixture through centrifugation. The Ag nanocube solution was then dispersed in 10 mL of ethanol and 100 mL of aqueous poly(vinylpyrrolidone) solution (0.2 g/L). The resulting solution was vacuum filtered using Durapore polyvinylidene fluoride filter membranes (Millipore) with pore sizes ranging from 5000, 650, 450, to 220 nm and repeated several times for each pore size. The Ag nanocubes were then redispersed in ethanol (∼5 mg/mL) and stored in the refrigerator.

4-Methylbenzenethiol (4-MBT) Functionalization of Ag Nanocubes. The removal of surfactant from Ag nanocubes surface was done by functionalizing the assembled Ag nanocubes with 4-MBT. The assembled Ag nanocube array was immersed in 5 mM of 4-MBT methanolic solution for at least 3 h.

HCl Treatment of Ag Nanocubes. The removal of surfactant from the Ag nanocube surface was referred to the method in literature.[2] This is to provide a featureless SERS background in the region of 600 to 1700 cm^{-1} which is necessary for accurate analyte detection. a 100 μL portion of purified Ag nanocubes in ethanol suspension (10 mg/mL) was added to 5 mL of hydrochloric acid (0.01 M) in water under stirring conditions. After 3 h, the Ag nanocube colloidal suspension was then washed with copious amounts of pure water and ethanol to remove excess HCl. The HCl-treated Ag nanocubes were subsequently redispersed in ethanol for further use. *Either 4-MBT functionalization or HCl treatment can remove the surfactants. Nonetheless, 4-MBT functionalization will form a layer of 4-MBT probe on the surface. This is for characterization or detection experiment that needs 4-MBT signals as "internal" standards to base on. HCl treatment will only remove the surfactant and leave a clean surface. This is for experiments where "internal" 4-MBT signals are not required, such as the detection of 4-MBT, toluene, or naphthalene from the external environment.

Synthesis of Ag@ZIF Core−Shell. A 250 μL portion of $Zn(NO_3)_2$ (25 mM) was added to a vial of 1.3 mL of methanol and stirred at 500 rpm for 5 min. A 250 μL portion of methanolic 2-methylimidazole (50 mM) was then added, followed by the immediate addition of 200 μL of Ag nanocubes solution (4.7 mg/mL, Ag nanocubes can be functionalized with 4-MBT to have 4-MBT probe internal standard or HCl-treated to remove surface groups). The mixture was stirred for another 90 min at 500 rpm. Excess reagents were removed by centrifugation, and the core−shell nanocubes were then washed twice with methanol and then finally redispersed in methanol.

Assembly of Ag@MOF Nanocubes into Multilayered Substrates (Substrate 1/Ag@MOF Substrate). Briefly, 0.5 cm × 0.5 cm Si (100) substrates were cleaned prior to assembly of Ag@MOF using oxygen plasma (FEMTO SCIENCE, CUTE-MP/R, 100 W) for 5 min. Twenty microliters of the 1-propanol solution of Ag@MOF particles (with concentration of 0.5−20 mg/mL for different Ag@MOF thickness) was dispensed *via* pipet on the substrates and allowed dry. It is noteworthy to mention that the concentration of Ag@MOF particles required also varies when used on varying areas of Si substrates for the same Ag@MOF thickness. For example, if a larger substrate is used, a higher concentration of Ag@MOF particles is required to obtain the same thickness.

Multilayered Ag Nanocube Substrate and Growth of Zeolitic Imidazolate Framework-8 (ZIF) Film on Multilayered Ag Nanocube Substrate (Substrates 3 and 2). Briefly, 0.5 cm × 0.5 cm Si (100) substrates were cleaned prior to assembly of Ag nanocubes using oxygen plasma (FEMTO SCIENCE, CUTE-MP/R, 100 W) for 5 min. Twenty microliters of the 1-propanol solution of Ag nanocubes (after filtration, with concentration of 0.5−20 mg/mL) was dispensed *via* pipet on the substrates and allowed dry. The coated substrate was submerged in hydrochloric acid (0.01 M) for 3 h to remove PVP surface groups on Ag nanocubes. Multilayered Ag nanocube substrate (substrate 3) was obtained.

For substrate 2 preparation, ZIF coating was performed. A 2 mL portion of methanolic $Zn(NO_3)_2$ (25 mM) was added to 2 mL of methanolic 2-methylimidazole (mIM; 50 mM) and mixed quickly for 5 s. For one growth cycle, the Ag nanocube substrate (9−10 layers, ∼5 mg/mL Ag nanocube solution was used) was immersed in the solution for 40 min and then washed with copious amount of methanol and dried with nitrogen gas several times to remove excess ZIF crystals. The procedure was repeated two more times using fresh $Zn(NO_3)_2$ and 2-methylimidazole solutions to obtain ZIF film of ∼200 nm (standardized Ag/MOF ratio with Ag@MOF platform). The ZIF film on the multilayered Ag nanocube substrate achieves a thickness of 1.3 μm with ∼10 layers of Ag cube and 200 nm MOF, which is standardized with the Ag@MOF substrate of 1.3 μm with ∼12 layers of Ag@MOF cube.

Activation of Substrates. All MOF-modified substrates were thermally activated to remove any solvent molecules within its pores by heating the substrate under vacuum at 120 °C for 2 h. The substrates were used immediately after activation.

Preparation of 3D-Printed Chamber for Airborne Chemicals. 3D models were designed in AutoDesk 3Ds Max 2016, and exported to and printed with FormLabs 1+ 3D printer using clear resins FL02. The chamber was designed such that the airborne analyte can be sprayed into from top down. The chamber interior and the laser source (objective lens) were separated with a quartz slide to limit chemical dispersion in laboratory-based exeperiments. For outdoor experiments, the quartz slide was removed to minimize loss of laser power and signal intensity.

DOI: 10.1021/acsnano.9b06486
ACS Nano 2019, 13, 12090−12099

SERS Detection of Aerosolized Chemicals. Solutions of analytes were loaded into commercially available "Nano Handy Mist Spray" (SKG brand) and expelled out as aerosols. Typically, our measurement estimates that 1 s of spraying produces a total of 50 μL of airborne aerosol. Aerosols were introduced into the chamber in which the SERS platforms are mounted at one side of the walls. Stand-off SERS measurement was performed *in situ* for the entire duration (before, during, and after spraying of airborne analytes). SERS spectra were obtained with time-lapsed mode every 1 s with 1 s collection time—for characterization of 4-MBT premodified substrates or every 10 s with 10 s collection time—for detection of airborne 4-MBT. About 5−10 SERS spectra were averaged and baselined for each analyte concentration. To measure the distance-dependent signal intensity at different distances, the measurement was performed as the substrate was positioned at 2 m to 4, 6, 8, and 10 m away from the lens (Figure S11). Spectra when the substrate was saturated (maximum intensity) were analyzed for intensity.

SERS Detection of Gaseous 4-MBT. Instead of aerosolized 4-MBT, 0.5 g of solid 4-MBT was put in the chamber. Stand-off SERS measurements were performed *in situ* as the solid sublimed. SERS spectra were obtained with time-lapsed mode every 10 s with 10 s collection time. To determine the penetration depth of gaseous 4-MBT (Figure 1B), the substrates were collected after 2 h and subjected to confocal $x-z$ hyperspectral imaging.

SERS Detection of CO_2 in Gas Detector. The thermal-activated SERS platforms were placed inside a custom-made gas flow cell for SERS examination. The gas flow cell was first flushed with N_2 gas (50 sccm) for 30 min to displace air from our experimental setup. Following this, CO_2 gas (50 sccm) was flown through the gas flow cell and stopped after 15−20 min. The cell was then vacuumed for 15−20 min. CO_2 gas (50 sccm) was flown through again, and the cycle was repeated. Stand-off SERS measurement was performed *in situ* for the entire duration (time-lapsed mode every 5 min with 30 s collection time). Subsequent purging of the experimental setup with N_2 gas and simultaneous SERS analysis were conducted until characteristic SERS bands remained constant in the SERS spectra (30 min). All gas flows were precisely controlled using precision gas mass flow controllers (model no. MC-100SCCM-D) obtained from Alicat Scientific, Inc. All SERS spectra were normalized between 0 (min) and 1 (max), and their SERS intensities (I) were based on the relative intensity of 4-MBT internal standard.

Stand-off Outdoor Experiment. The experiment was performed in daytime before 5 pm (Singapore time) at the level 6 (rooftop) open area within the Division of Chemistry and Biological Chemistry, School of Physical and Mathematical Sciences, NTU. The experimental procedures for the detection of aerosolized analytes were performed accordingly to laboratory-based experiments.

Characterization. Scanning electron microscope (SEM) imaging was performed using a JEOL-JSM-7600F microscope. SEM images of Ag@MOF particles are overlapping images of two sets of images with the same magnification, taken with (1) secondary electron imaging (SEI) mode, which reveals the MOF coating, and (2) low-angle backscattered electrons (LABE) mode, which reveals the Ag core, to fully visualize the core−shell structure in 3D. The titled SEM image was performed at a 10° tilt angle (Figure 1A(ii)). Transmission electron microscope (TEM) imaging was performed using JEOL-2100 at an accelerating voltage of 200 kV. UV−vis spectra were measured with Cary 60 UV−vis spectrometer. Substrate X-ray diffraction patterns were recorded on a Bruker GADDS XRD diffractometer with Cu Kα radiation. Stand-off SERS was performed on a portable stand-off Raman spectrophotometer with a mounted 200 mm Nikon lens, at ≤55 mW laser power, 532 nm wavelength, 1 mm × 1 mm × 3.9 mm laser volume (Technospex Pte. Ltd., Singapore). Hyperspectral SERS imaging were performed using $x-y$, $x-z$, and $x-y-z$ hyperspectral imaging mode of the Ramantouch microspectrometer (Nanophoton Inc., Osaka, Japan) with an excitation wavelength of 532 nm and laser power of 0.06 mW. A 100× objective lens (N.A 0.90), 20× objective lens (N.A 0.45), and 4× objective lens (N.A 0.13, for large scale imaging) with 1 s acquisition time was used for data collection. For $x-y-z$ image (Figure 1A(iii)), original data were obtained over 400 horizontal pixels and cropped to ∼150 horizontal pixels. All confocal and stand-off SERS spectra are subjected to background subtraction and baseline correction.

ASSOCIATED CONTENT

Supporting Information

The Supporting Information is available free of charge on the ACS Publications website at DOI: 10.1021/acsnano.9b06486.

Supporting figures, supporting discussion and calculations describing the preparation of multilayered substrates, their characterization and the stand-off measurements (PDF)

Spraying aerosolized chemicals into the vicinity of Ag@MOF platform for stand-off sensing (MOV)

Outdoor real-time stand-off SERS sensing of airborne chemicals (MOV)

AUTHOR INFORMATION

Corresponding Authors

*E-mail: xyling@ntu.edu.sg.

*E-mail: phangiy@imre.a-star.edu.sg.

ORCID

Yue-E Miao: 0000-0002-3660-029X

Wei Fan: 0000-0001-6978-1405

Xing Yi Ling: 0000-0001-5495-6428

Notes

The authors declare no competing financial interest.

ACKNOWLEDGMENTS

X.Y.L. thanks the Singapore Ministry of Education Tier 1 (RG11/18) and Tier 2 (MOE2016-T2-1-043) grants. G.C.P.-Q. and C.S.L.K. are thankful for Nanyang President's Graduate Scholarships. N.Y. is thankful for the CN Yang scholarship. T.L. acknowledges the funding support from the National Natural Science Foundation of China (51433001).

REFERENCES

(1) Fan, M.; Andrade, G. F. S.; Brolo, A. G. A Review on the Fabrication of Substrates for Surface Enhanced Raman Spectroscopy and Their Applications in Analytical Chemistry. *Anal. Chim. Acta* **2011**, *693*, 7−25.

(2) Hobro, A. J.; Lendl, B. Stand-Off Raman Spectroscopy. *TrAC, Trends Anal. Chem.* **2009**, *28*, 1235−1242.

(3) Chou, A.; Jaatinen, E.; Buividas, R.; Seniutinas, G.; Juodkazis, S.; Izake, E. L.; Fredericks, P. M. SERS Substrate for Detection of Explosives. *Nanoscale* **2012**, *4*, 7419−7424.

(4) Koh, C. S. L.; Lee, H. K.; Han, X.; Sim, H. Y. F.; Ling, X. Y. Plasmonic Nose: Integrating the MOF-Enabled Molecular Preconcentration Effect With APlasmonic Array For Recognition of Molecular-Level Volatile Organic Compounds. *Chem. Commun.* **2018**, *54*, 2546−2549.

(5) Phan-Quang, G. C.; Lee, H. K.; Ling, X. Y. Isolating Reactions at the Picoliter Scale: Parallel Control of Reaction Kinetics at the Liquid−Liquid Interface. *Angew. Chem., Int. Ed.* **2016**, *55*, 8304−8308.

(6) Carey, D. M.; Korenowski, G. M. Measurement of The Raman Spectrum of Liquid Water. *J. Chem. Phys.* **1998**, *108*, 2669−2675.

(7) Wallin, S.; Pettersson, A.; Östmark, H.; Hobro, A. Laser-Based Standoff Detection of Explosives: a Critical Review. *Anal. Bioanal. Chem.* **2009**, *395*, 259−274.

(8) Moros, J.; Lorenzo, J. A.; Novotný, K.; Laserna, J. J. Fundamentals of Stand-Off Raman Scattering Spectroscopy for Explosive Fingerprinting. *J. Raman Spectrosc.* **2013**, *44*, 121−130.

(9) Gopalsami, N.; Raptis, A. C. Millimeter-Wave Radar Sensing of Airborne Chemicals. *IEEE Trans. Microwave Theory Tech.* **2001**, *49*, 646−653.

DOI: 10.1021/acsnano.9b06486
ACS Nano 2019, 13, 12090−12099

(10) Mosier-Boss, P. A. Review of SERS Substrates for Chemical Sensing. *Nanomaterials* **2017**, *7*, 142.
(11) Lee, H. K.; Lee, Y. H.; Koh, C. S. L.; Phan-Quang, G. C.; Han, X.; Lay, C. L.; Sim, H. Y. F.; Kao, Y.-C.; An, Q.; Ling, X. Y. Designing Surface-Enhanced Raman Scattering (SERS) Platforms Beyond Hotspot Engineering: Emerging Opportunities in Analyte Manipulations and Hybrid Materials. *Chem. Soc. Rev.* **2019**, *48*, 731−756.
(12) Phan-Quang, G. C.; Lee, H. K.; Teng, H. W.; Koh, C. S. L.; Yim, B. Q.; Tan, E. K. M.; Tok, W. L.; Phang, I. Y.; Ling, X. Y. Plasmonic Hotspots in Air: An Omnidirectional Three-Dimensional Platform for Stand-Off In-Air SERS Sensing of Airborne Species. *Angew. Chem., Int. Ed.* **2018**, *57*, 5792−5796.
(13) Scaffidi, J. P.; Gregas, M. K.; Lauly, B.; Carter, J. C.; Angel, S. M.; Vo-Dinh, T. Trace Molecular Detection *via* Surface-Enhanced Raman Scattering and Surface-Enhanced Resonance Raman Scattering at a Distance of 15 Meters. *Appl. Spectrosc.* **2010**, *64*, 485−492.
(14) Lee, H. K.; Lee, Y. H.; Morabito, J. V.; Liu, Y.; Koh, C. S. L.; Phang, I. Y.; Pedireddy, S.; Han, X.; Chou, L.-Y.; Tsung, C.-K.; Ling, X. Y. Driving CO_2 to a Quasi-Condensed Phase at the Interface between a Nanoparticle Surface and a Metal−Organic Framework at 1 bar and 298 K. *J. Am. Chem. Soc.* **2017**, *139*, 11513−11518.
(15) Lee, M. R.; Lee, H. K.; Yang, Y.; Koh, C. S. L.; Lay, C. L.; Lee, Y. H.; Phang, I. Y.; Ling, X. Y. Direct Metal Writing and Precise Positioning of Gold Nanoparticles within Microfluidic Channels for SERS Sensing of Gaseous Analytes. *ACS Appl. Mater. Interfaces* **2017**, *9*, 39584−39593.
(16) Sharma, S. K. New Trends in Telescopic Remote Raman Spectroscopic Instrumentation. *Spectrochim. Acta, Part A* **2007**, *68*, 1008−1022.
(17) Phan-Quang, G. C.; Lee, H. K.; Phang, I. Y.; Ling, X. Y. Plasmonic Colloidosomes as Three-Dimensional SERS Platforms with Enhanced Surface Area for Multiphase Sub-Microliter Toxin Sensing. *Angew. Chem., Int. Ed.* **2015**, *54*, 9691−9695.
(18) Lee, H. K.; Lee, Y. H.; Phang, I. Y.; Wei, J.; Miao, Y.-E.; Liu, T.; Ling, X. Y. Plasmonic Liquid Marbles: A Miniature Substrate-Less SERS Platform for Quantitative and Multiplex Ultratrace Molecular Detection. *Angew. Chem., Int. Ed.* **2014**, *53*, 5054−5058.
(19) Sim, H. Y. F.; Lee, H. K.; Han, X.; Koh, C. S. L.; Phan-Quang, G. C.; Lay, C. L.; Kao, Y.-C.; Phang, I. Y.; Yeow, E. K. L.; Ling, X. Y. Concentrating Immiscible Molecules at Solid@MOF Interfacial Nanocavities to Drive an Inert Gas−Liquid Reaction at Ambient Conditions. *Angew. Chem., Int. Ed.* **2018**, *57*, 17058−17062.
(20) Yin, H.; Kim, H.; Choi, J.; Yip, A. C. K. Thermal Stability of ZIF-8 Under Oxidative and Inert Environments: A Practical Perspective on Using ZIF-8 as ACatalyst Support. *Chem. Eng. J.* **2015**, *278*, 293−300.
(21) Lee, Y. H.; Lay, C. L.; Shi, W.; Lee, H. K.; Yang, Y.; Li, S.; Ling, X. Y. Creating Two Self-Assembly Micro-Environments to Achieve Supercrystals With Dual Structures Using Polyhedral Nanoparticles. *Nat. Commun.* **2018**, *9*, 2769.
(22) Rauh, A.; Rey, M.; Barbera, L.; Zanini, M.; Karg, M.; Isa, L. Compression of Hard Core−Soft Shell Nanoparticles at Liquid−Liquid Interfaces: Influence of The Shell Thickness. *Soft Matter* **2017**, *13*, 158−169.
(23) Chen, M.; Phang, I. Y.; Lee, M. R.; Yang, J. K. W.; Ling, X. Y. Layer-By-Layer Assembly of Ag Nanowires into 3D Woodpile-Like Structures to Achieve High Density "Hot Spots" for Surface-Enhanced Raman Scattering. *Langmuir* **2013**, *29*, 7061−7069.
(24) Li, X.; Lee, H. K.; Phang, I. Y.; Lee, C. K.; Ling, X. Y. Superhydrophobic-Oleophobic Ag Nanowire Platform: An Analyte-Concentrating and Quantitative Aqueous and Organic Toxin Surface-Enhanced Raman Scattering Sensor. *Anal. Chem.* **2014**, *86*, 10437−10444.
(25) Kodiyath, R.; Malak, S. T.; Combs, Z. A.; Koenig, T.; Mahmoud, M. A.; El-Sayed, M. A.; Tsukruk, V. V. Assemblies of Silver Nanocubes for Highly Sensitive SERS Chemical Vapor Detection. *J. Mater. Chem. A* **2013**, *1*, 2777−2788.
(26) Qualey, J. R. Fire Test Comparisons of Smoke Detector Response Times. *Fire Technol.* **2000**, *36*, 89−108.
(27) Cleary, T. Results from a Full-Scale Smoke Alarm Sensitivity Study. *Fire Technol.* **2014**, *50*, 775−790.
(28) Oh, M.-K.; De, R.; Yim, S.-Y. Highly Sensitive VOC Gas Sensor Employing Deep Cooling of SERS Film. *J. Raman Spectrosc.* **2018**, *49*, 800−809.
(29) Cao, R.; Zhang, H.; Geng, N.; Fu, Q.; Teng, M.; Zou, L.; Gao, Y.; Chen, J. Diurnal Variations of Atmospheric Polycyclic Aromatic Hydrocarbons (PAHs) During Three Sequent Winter Haze Episodes in Beijing, China. *Sci. Total Environ.* **2018**, *625*, 1486−1493.

DOI: 10.1021/acsnano.9b06486
ACS Nano 2019, 13, 12090−12099